CEBAF-ER: EXTENDING THE FRONTIER OF
ENERGY RECOVERY AT JEFFERSON LAB[*]

C. Tennant[#], K. Beard, A. Bogacz, Y. Chao, S. Chattopadhyay, D. Douglas, A. Freyberger,
A. Hutton, L. Merminga, M. Tiefenback, H. Toyokawa
Thomas Jefferson National Accelerator Facility, Newport News, VA 23606, USA

Abstract

A successful GeV scale energy recovery demonstration with a high ratio of peak-to-injection energies (50:1) was recently carried out on the CEBAF (Continuous Electron Beam Accelerator Facility) recirculating superconducting linear accelerator in an effort to address issues related to beam quality preservation in a large scale energy recovery system. To gain a quantitative understanding of the beam behavior through the machine, an intense effort was made to characterize the 6D phase space during the CEBAF-ER (CEBAF with Energy Recovery) experimental run. A scheme was implemented to measure the transverse emittance of the energy recovered beam prior to being sent to the dump, as well as in the injector and in each arc. The emittance provides a figure of merit in this context inasmuch as it characterizes the extent to which beam quality is preserved during energy recovery. In addition to describing the transverse phase space, the momentum spread was measured in the injector and arcs to characterize the longitudinal phase space. Measurements also included the RF system's response to the energy recovery process. And by using a novel technique employing wire scans in conjunction with PMTs (Photomultiplier Tubes) to accurately measure the beam profile at the dump, we can qualitatively characterize beam preservation through the recirculator. One of the salient conclusions from the experiment is that the energy recovery process does not contribute to the emittance degradation since the emittance of the recirculating pass is consistent with that of the accelerating pass.

INTRODUCTION AND MOTIVATION

The purpose of energy recovery is to recycle the electron beam energy, which is produced by accelerating electrons in electromagnetic fields, and reuse the energy. The principle of energy recovery in a recirculating RF (radio frequency) linac is based on the fact that the RF fields, by proper choice of the time-of-arrival of the electron bunches in the linac beam, may be used to both accelerate and decelerate the same beam. Consider the simplest case of a single recirculation. Beam is injected into the linac and timed to accelerate on the first pass up the linac. If the recirculation path is chosen to be precisely an integer plus ½ RF wavelengths, on the second pass through the linac, the beam is actually *decelerated* by the same RF field which accelerated it on the first pass. For cavities within the recirculation loop, energy is directly transferred, via the RF field, from decelerating beam to accelerating beam. The key point is that these RF power systems do not need to provide the energy to accelerate the first pass beam. Indeed, the RF power draw becomes almost completely independent of the beam current. Power demands are further diminished by utilizing superconducting RF cavities - whose high Q-values ensure minimal wall losses [1].

High energy (multi-GeV), high current (hundreds of milli-Amperes) beams require gigaWatt-class RF systems in conventional linear accelerators - a prohibitively expensive proposition. However, invoking energy recovery alleviates extreme RF power demands, improves linac efficiency and increases cost effectiveness. Jefferson Lab has demonstrated its expertise in the field of energy recovery linacs (ERLs) with the successful operation of the infrared free electron laser (IR FEL), where 5 mA of average beam current have been accelerated up to 50 MeV and the energy stored in the beam was recovered via deceleration and given back to the RF power source [2]. To date the FEL is the highest beam power demonstration of energy recovery.

Presently there are proposals for several ERL based accelerator systems world-wide. These include designs for FELs (KAERI), synchrotron light sources (Cornell/JLab ERL, ERLSYN, 4GLS, BINP MARS), electron cooling devices (BNL-BINP) and electron-ion colliders (ELIC, eRHIC) [3]. Some of the ERL-based accelerator applications that are being proposed require beam currents of the order of 100 mA, while the beam energy for these applications ranges from the currently achieved 50 MeV up to 5 GeV.

There are several important accelerator physics and technological issues that must be resolved before any of these applications can be realized. The JLab FEL upgrade (presently being commissioned) designed to accelerate 10 mA up to 150 MeV and then energy recovered, and the proposed Cornell/Jlab ERL Prototype, designed to accelerate 100 mA up to 100 MeV and then decelerated for energy recovery will be ideal test beds for the understanding of high current phenomena in ERL devices. In an effort to address the issues of energy recovering high energy beams, Jefferson Lab proposed a minimally invasive energy-recovery experiment utilizing the CEBAF accelerator [4]. The experiment commenced in late March with the goal of demonstrating the energy recovery of a 1 GeV beam while characterizing the beam phase space at various points in the machine and measuring the RF

system's response to energy recovery. Once satisfactory measurements were obtained using the nominal 55 MeV injection energy, the measurements were repeated for low injection energy (20 MeV) to study the parametric dependence on low injection to final energy ratios. Until this experiment, there were no plans aimed to address issues related to beam quality preservation in systems with large final beam energy (up to 1 GeV) or large energy ratio between final and injected beams (up to a factor of 50).

THE EXPERIMENT

General Layout

A schematic representation of the CEBAF-ER experiment is illustrated in Figure 2. Beam is injected into the North Linac at 55 MeV where it is accelerated to 555 MeV. The beam traverses Arc 1 and then begins acceleration through the South Linac where it reaches a maximum energy of 1055 MeV. Following the South Linac, the beam passes through a newly installed phase delay chicane. The chicane was designed to create a path length differential of exactly ½-RF wavelength so that upon re-entry into the North Linac, the beam is 180° out of phase with the respect to the cavities and will subsequently be decelerated to 555 MeV. After traversing Arc 1 the beam enters the South Linac - still out of phase with the cavities - and is decelerated to 55 MeV at which point the spent electron beam is sent to a dump. In this way the beam gives energy back to the RF system, which is used to accelerate subsequent beam.
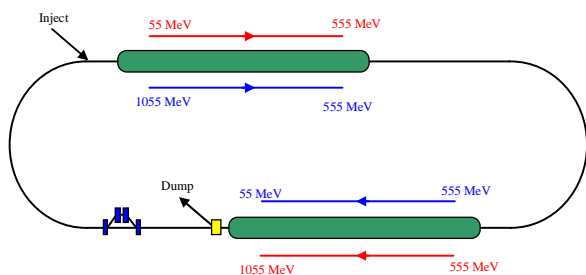

Figure 2: CEBAF-ER schematic layout.

Beam Transport – Linac Optics

The linac optics were optimized for the two co-propagating beams so that the lower energy beam in each linac had a 120° betatron phase advance per cell lattice, as illustrated by the beta functions in Figures 3 and 4 (the vertical scale is 300 m and β_x = red, β_y = green). Appropriate optics design for the spreader and recombiner of Arc 2 (following South Linac) facilitates compensation of beta mismatches introduced by optimizing the linac optics for the lower energy beam.
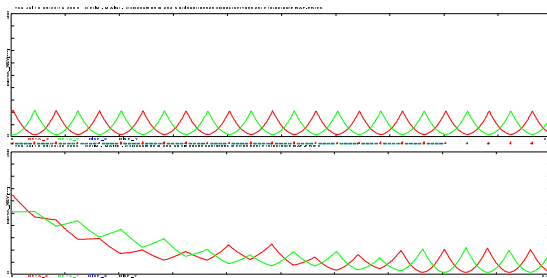

Figure 3: North Linac ̃ top: Betatron functions of 120° per cell lattice for the accelerating beam and bottom: mismatched optics for the decelerating beam.
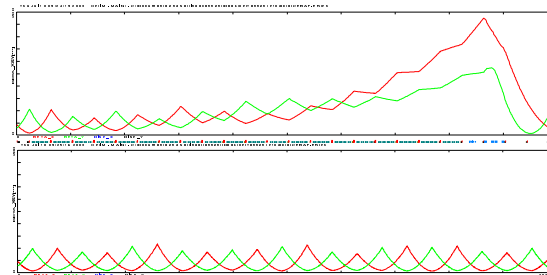

Figure 4: South Linac ̃ top: Betatron functions of the mismatched optics for the accelerating beam and bottom: 120° per cell lattice for the decelerating beam.

Successful Energy Recovery

On March 26, 2003, 7µA of pulsed beam, accelerated to 1055 MeV and energy recovered at 55 MeV, was successfully steered to the beam dump. Figure 5 displays the beam at various locations through CEBAF. The rightmost image shows the two co-propagating beams as seen by the synchrotron light monitor (SLM) in Arc 1. The upper image is that seen by a beam viewer located approximately half way through the South Linac, where once again, we have two beams. The final image is that from the optical transition radiation (OTR) camera on the beam dumpline which indicates we have successfully energy recovered. The bottom image shows the phase delay chicane installed for the experiment.

PHASE SPACE MEASUREMENTS

To gain a quantitative understanding of the beam behavior through the machine, an intense effort was made to characterize as much of the 6D phase space as possible during the CEBAF-ER experimental run [5]. A scheme has been implemented to measure the transverse emittance of the energy recovered beam prior to being sent to the dump, as well as in the injector and in each arc. In this way we can understand how the emittance evolves through the machine. In addition to describing the transverse phase space, the momentum spread was measured in the injector and arcs to characterize the longitudinal phase space.
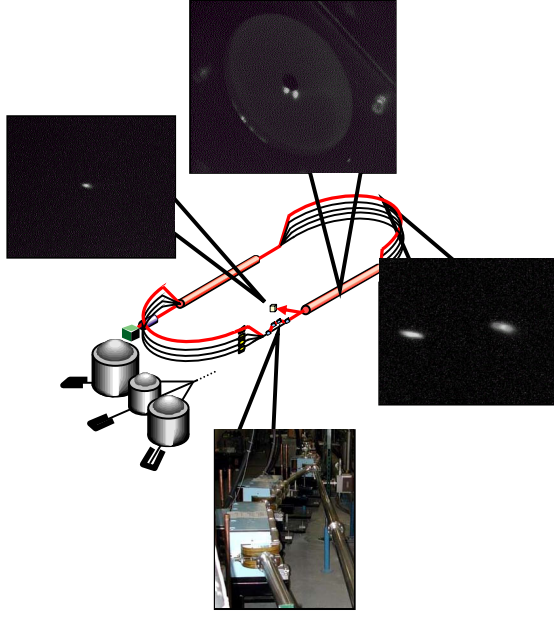
Figure 5: Beam spots on various monitors the during CEBAF-ER experiment.

Emittance and Momentum Spread in the Injector and Arcs

The emittance and momentum spread of the first pass beam were measured in the injector, Arc 1, and Arc 2 utilizing a scheme involving multiple optics and multiple wire scanners. Two wire scanners were placed in each arc, one at the beginning of the arc in a non-dispersive region and the second in the middle of the arc at a point of high dispersion (6 m). The emittance in the injector was measured using five wire scanners along the injector line. The results of the momentum spread measurements are given in Table 1 and the emittance measurements are shown in Figures 10 and 11.

Location	$\sigma p/p$ (10^{-3})	E_{beam} (MeV)	$\sigma p/p$ (10^{-3})	E_{beam} (MeV)
Injector (1st pass)	0.0290 ($\pm$ 0.0096)	55	0.0369 ($\pm$ 0.0010)	20
Arc 1 (1st pass)	0.0079 ($\pm$ 0.0023)	555	0.0071 ($\pm$ 0.0010)	520
Arc 2 (1st pass)	0.0198 ($\pm$ 0.0018)	1055	0.0100 ($\pm$ 0.0014)	1020

Table 1: Measured fractional energy spread.

Emittance in the Extraction Region

Of great interest is the beam emittance of the energy recovered beam prior to delivery to the dump. Whereas the previous section described the use of multiple wire scanners and multiple optics to obtain the emittances in the injector and Arcs, the emittance in the extraction region relied on a single scanning quadrupole and a wire scanner. The quadrupole at region 2L21 (just after the exit of the South Linac) was scanned and used to obtain the emittance in the horizontal plane while the adjacent, downstream quad at 2L22 was scanned to obtain the vertical emittance. Because of the presence of the two co-propagating beams in the extraction region (the first pass beam at 1055 MeV and the second pass, energy recovered beam at 55 MeV), care was taken to produce compensatory optics using a family of downstream quads to ensure the first pass beam would be unaffected and transported through the machine.

By the end of the CEBAF-ER run, data were collected to calculate the emittance in each transverse plane for injection energies of 55 and 20 MeV. All the analysis was done off-line. First, the signals of the raw wire scans were fit with a Gaussian distribution and the sigmas of each extracted. For the case of a quadrupole-drift-wire scanner configuration, one can show that the beam size squared depends quadratically on the quadrupole strength,

$$\sigma^2_{measured} = \beta_{wire}\varepsilon = (1+kL)^2(\beta_{quad}\varepsilon) - 2L(1+kL)(\alpha_{quad}\varepsilon) + L^2(\gamma_{quad}\varepsilon)$$

where L is the distance from the quadrupole to the wire scanner and k is the quadrupole strength in the thin lens approximation. By plotting the sigmas squared versus the M_{11} element and performing a least-squares fit, the emittance as well as the Twiss functions at the entrance of the scanning quadrupole can be extracted as shown in Figure 6 [6].
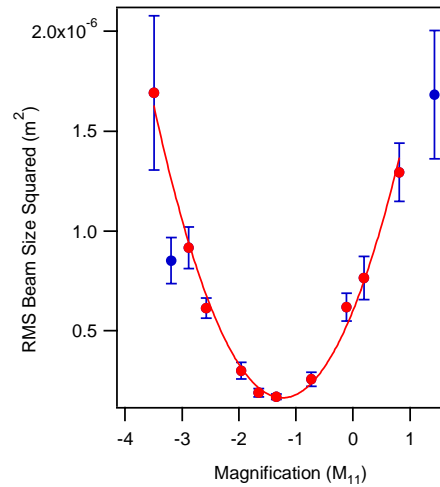

Figure 6: Beam size squared vs M_{11}.

BEAM PROFILE MEASUREMENTS

Wire scanners are used throughout the CEBAF accelerator to measure the beam profile. The wire scanner mechanism drives 25 μm tungsten wires through the electron beam, oriented in the X, XY and Y axes. The standard CEBAF wire scanner measures the induced current on the wire due to secondary emission of electrons from the wire. These induced currents tend to be in the nA range and this system is well suited to measuring the core σ of beam and have a dynamic range of about 100. To improve on the dynamic range of the wire scanner for beam profile measurements of the energy recovered beam, instrumentation was added to the wire scanner just upstream of the beam dump. This instrumentation relies on photomultiplier tubes to detect the scattered electron or the subsequent shower from the incident beam intercepting the wire [7]. The beam currents for the energy recovery experiment are large (tens of μA) compared to those previously measured using this method in CEBAF's Hall-B (nA range) where photomultipliers are used routinely.

The beam profiles for the energy recovered beam are processed in a manner similar to that described in Reference [7]. Instead of merging data from wires of different diameters, the photomultipliers were operated with different gains. The data are combined to yield a beam profile with greater dynamic range than one would obtain using a single photomultiplier or by measuring the induced current on the wire. Fits were performed with the data. The Y (vertical) profile for both the 55 MeV and 20 MeV recovered beam are well represented by a single Gaussian over the complete (5 to 6 orders of magnitude) dynamic range. The X (horizontal) profile for the 55 MeV beams shows a small additional contribution on the left side of the plot, perhaps due to beam scraping (see Figure 7). The broader width of the X profile at 20 MeV is explained by the fact that the measurement was located in a region of dispersion and is therefore scaled by a factor of $\Delta E/E$ (see Figure 8). This may account for the observed increase in horizontal scraping when operating with an injection energy of 20 MeV.
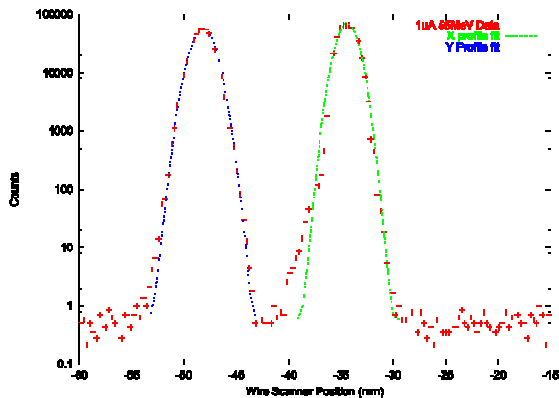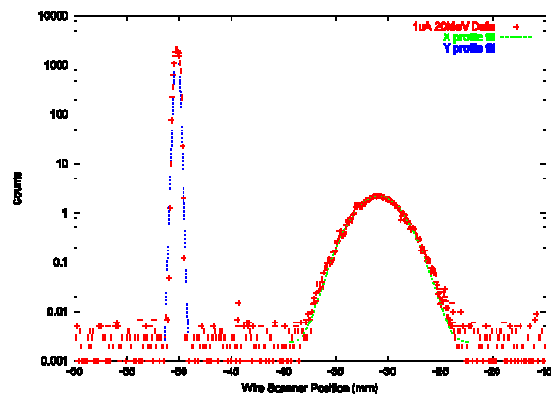

Figure 8: Large dynamic range X and Y beam profile measurements of energy recovered beam with E=20 MeV.

RF MEASUREMENTS

In addition to the beam based measurements presented in the previous sections, another important class of measurements deals with the RF system's response to energy recovery [8]. As an example, consider Figure 9 which illustrates the RF system gradient modulator drive signal during pulsed beam operation. Without energy recovery this signal is nonzero when a 250 μs beam pulse enters the RF cavity, indicating power is drawn from the cavity. With energy recovery, the signal is zero once the initial transient passage of the leading edge of the pulse is over, indicating no additional power draw is required by the cavity.
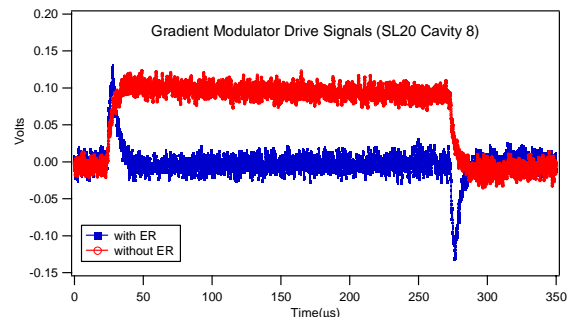

Figure 9: Gradient modulator drive signals during pulsed beam operation with and without energy recovery.

PRELIMINARY CONCLUSIONS

One of the most important sets of measurements was of the transverse emittance shown in Figures 10 and 11. The plots display the measured emittances at locations throughout CEBAF; specifically the data points (from left to right) are the emittance in the injector, Arc 1, Arc 2 and upon exiting the South Linac on the second pass, respectively. The emittances for each injection energy are remarkably consistent except for the Arc 2 data point with E_{inj} = 55 MeV. This is currently a topic of investigation. Clearly the emittance is degraded by passage through the linacs. Possible causes are [9] cavity fundamental power coupler dipole mode driven steering and cavity higher order mode coupler induced transverse coupling.

Figure 7: Large dynamic range X and Y beam profile measurement of energy recovered beam with E=55 MeV.

Estimates suggest that the horizontal projected emittance could grow by a factor of 2 due to the effects of dipole mode head-tail steering [10].

Perhaps the most significant conclusion is that the energy recovery process does not contribute significantly to the emittance degradation since the emittance of the recirculating pass is consistent with that of the accelerating pass. Furthermore, as a result of the CEBAF-ER experiment, the following were achieved:

- Demonstrated the feasibility of energy recovering a *high energy* (1 GeV) beam through a *large* (~1 km circumference), *superconducting* (320 cavities) machine.
- 80 μA of cw beam, accelerated to 1055 MeV and energy recovered at 55 MeV, was steered to the ER dump.
- 1 μA of cw beam, accelerated to 1020 MeV and energy recovered at 20 MeV, was steered to the ER dump.
- Tested the dynamic range on system performance by demonstrating high final-to-injector energy ratios (E_{final}/E_{inj}) of 20:1 and 50:1.
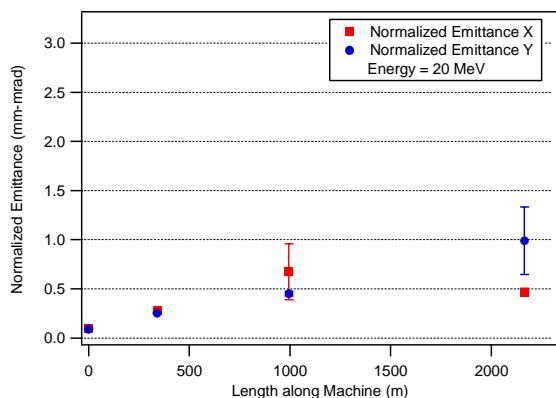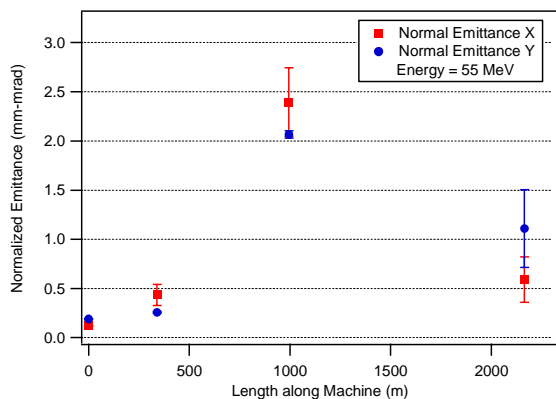

Figure 10: Emittance evolution for E_{inj} = 20 MeV.

Figure 11: Emittance evolution for E_{inj} = 55 MeV.

REFERENCES

[1] L. Merminga, D. Douglas, G. Krafft, "High Current Energy Recoverying Electron Linacs" Annu. Rev. Nucl. Part. Sci., **53**, 387 (2003).

[2] G. Neil, et. al., "Sustained Kilowatt Lasing in a Free-Electron Laser with Same-Cell Energy Recovery" Phys. Rev. Lett., **84** , 662 (2000).

[3] L. Merminga, et. al., *op. cit.*

[4] A. Bogacz, et. al., "CEBAF Energy Recovery Experiment - Proposal", JLAB-TN-03-006, (2002).

[5] C. Tennant, et. al., "Beam Characterization in the CEBAF-ER Experiment", Proceedings of Particle Accelerator Conference (2003).

[6] C. Tennant, "An Overview of Emittance Measurements in CEBAF-ER", TN-03-004 (2003).

[7] A. Freyberger, "Large Dynamic Range Beam Profile Measurements" Proceedings of Particle Accelerator Conference (2003).

[8] C. Tennant, et. al., "CEBAF-ER: An Experiment for Large Scale Demonstration of Energy Recovery" ICFA Beam Dynamics Newsletter, No. **30** (2003).

[9] Z. Li, "Beam Dynamics in the CEBAF Superconducting Cavities", Ph.D Thesis, College of William and Mary (1995).

[10] R. York, C. Reece, "RF Steering in the CEBAF CW Superconducting Linac", Proceedings of Particle Accelerator Conference (1997).